



HAL
open science

A new empirical model for enhancing well log permeability prediction, using nonlinear regression method: Case study from Hassi-Berkine oil field reservoir – Algeria

H.E. Belhouchet, M.S. Benzagouta, A. Dobbi, A. Alquraishi, Joelle Duplay

► **To cite this version:**

H.E. Belhouchet, M.S. Benzagouta, A. Dobbi, A. Alquraishi, Joelle Duplay. A new empirical model for enhancing well log permeability prediction, using nonlinear regression method: Case study from Hassi-Berkine oil field reservoir – Algeria. *Journal of King Saud University - Engineering Sciences*, 2021, 33 (2), pp.136-145. 10.1016/j.jksues.2020.04.008 . hal-03364222

HAL Id: hal-03364222

<https://hal.science/hal-03364222>

Submitted on 4 Oct 2021

HAL is a multi-disciplinary open access archive for the deposit and dissemination of scientific research documents, whether they are published or not. The documents may come from teaching and research institutions in France or abroad, or from public or private research centers.

L'archive ouverte pluridisciplinaire **HAL**, est destinée au dépôt et à la diffusion de documents scientifiques de niveau recherche, publiés ou non, émanant des établissements d'enseignement et de recherche français ou étrangers, des laboratoires publics ou privés.

A New Empirical Model for Enhancing Well Log Permeability Prediction, Using Nonlinear regression method: Case study from Hassi-Berkine Oil Field Reservoir – Algeria

BELHOUCHE H.E., BENZAGOUTA M.S., DOBBI A., ALQURAIHI A., DUPLAY J.

Abstract

The reservoir permeability (K) factor is the key parameter for reservoir characterization. This parameter is considered as a determinant reservoir quality index. Depending on the data required and procedure availability, permeability can be defined from several methods such as; well test interpretation, wireline formation tester, and core data. These approaches can also be in assumption with permeability prediction targeting the non-cored sections. According to a similar status, well logs records can be an interesting support tool in use to reach the planned objectives. Thus, this investigation consists of finding out a model able to estimate the well log permeability and adjusting the outcome to the core permeability results.

In this led research, the applied approach to the core data, to start with, was aimed to determine the reservoir rock types (RRT) using the flow zone indicator (FZI) method. The obtained classification allows stating a permeability model for each rock type.

In order to calculate permeability from well logs, FZI has been founded out. A multi-regression technique was used to analyze the relationship of FZI with respect to specific logs such as Gamma-ray (GR), Density Log (RHOB), and Sonic log (DT). An objective function has been designated to minimize the quadratic error between the observed normalized FZI coming from core data, and the normalized FZI calculated from well logs. This process is carried out to identify a mathematical correlation allowing the estimation of FZI from porosity logs, leading to permeability determination. As results, permeability from logs was supporting relatively permeability defined from cores. The final results can be an accurate and real test for associating the exactitude performance of logging data records in boreholes with respect to the overall reservoir characterization sections. Thus, the applied investigation can be a genuine and quick method for essentially a specific deduction regarding the non-cored reservoir sections, with reference to rock typing, permeability and probably further reservoir factors.

Keywords

Permeability, Reservoir characterization, Rock typing, Hydraulic unite, Flow zone Indicator

1. Introduction

The development of an oil field is an entire range of research activities starting from exploration up to field development (Galard, Jean-Hector et Al., 2005). It consists of characterizing a sedimentary basin in detail. The exploration steps may involve seismic data, logging, and analysis up to geobodies identification. In order to get a stable, consistent and coherent model, specific studies have been developed (Al-Hajeri, M. et al., 2009). Dynamic modeling with reservoir fluid characterization, SCAL studies, and identification of initial conditions are also part of these orientations (Holtz, M. H., 2002). The reservoir characterization parameters in that purpose can be figured out by factors such as seismic attributes, rock typing and geostatic. These parameters concern can be through probabilistic function responsible for uncertainties.

Different researches on that purpose have been led. However, investigations can be exposed to some risks. Doubts can be issued from a reduction of exploration uncertainties and inefficiency related to the predicted potential and real reserves presence of hydrocarbons (Richard C. Selley and Stephen A.

43 Sonnenberg, 2015). In addition, any exploration achievement can be related to significant geologic
44 elements processes and rock typing (Al-Hajeri, M. et al., 2009). Modeling system and fluid dynamics
45 behavior can be key factors suitable for the reservoir potential evaluation and recovery challenge
46 (Galard, Jean-Hector et Al., 2005).

47 The Rock typing is a process of rock classification based on mineralogical composition, grain size, shape
48 and pore size distribution (PSD). Rock typing – fluid interaction, with fluid dynamic behavior, and
49 capillary effect are of importance in this organization. In such circumstances, the envisaged process can
50 involve: integrating, analyzing and synthesizing the real data supplied from different borehole records
51 and cores analysis.

52 Other detailed parameters used, to define rock typing as part of the reservoir comprehension,
53 characterization for fluid circulation aptitude is the hydraulic flow units (HFU). Rock typing
54 classification can be allocated to the same dynamic properties, the same porosity, and permeability
55 correlations results, identical capillary pressure profile and the same relative permeability curves.
56 Similar characteristics are well supported by Shenawi, S. H. et al., (2009). The cited authors found that
57 Hydraulic Unit (HU) determination and use is providing a useful and interesting advice and device for
58 rock typing definition in relation to the porous media assessment.

59 Once the rock typing identification procedure is done, reliable estimated permeability can be extended
60 to the non-cored wells. This assumption allows the generation of water saturation models and
61 minimizing convergence problems. Therefore, the reservoir performance is then related to generating
62 simulation sensitivities, involving possible rock classes endorsed by considered scaled field.
63 Accordingly, figuring out reservoir properties, it can be carried out along the whole reservoir sections.

64 Therefore, the requirement of conceptual studies in that regard is in need of sensitive steps materializing
65 the stability and convergence of the model as a digital one. For the case study, the reservoir
66 characterization, based on permeability (K) determination will lead to developing an operational
67 modeling device. This application is capable of calculating the permeability as a function of porosity
68 and lithology (Enaworu, E. et al., 2016). The impact of the rock properties on the static and dynamic
69 behavior of the fluid circulation, related to rock typing, is another essential controlling factor to consider
70 (Attia, M. Attia and Shuaibu, Habibu , 2015).

71 Control on permeability prediction for rock typing determination is also related to the flow zone
72 indicator (FZI). It is known that the FZI parameter is directly associated to the hydraulic unit for
73 considered rock type as well as its porous media (Enaworu, E. et al., 2016). The method was proposed
74 to decrease the absolute error between defined permeability from cores and the calculated one. In
75 addition, applied method can ensure better development of the considered oilfield by optimizing the
76 perforation intervals. With regards to the overall, an enhancement boreholes recovery can be set.
77 Meanwhile, the method will guide avoiding the interval located in the aquifer section: Since
78 underestimation of the permeability in the section near the oil-water contact (OWC) can be considered
79 as the main issue for water breakthrough occurrence.

80 The preferred zone for perforation is generally carried out in interval above the oil-water contact. This
81 scenario is intended to delay the water breakthrough arrival. On the other hand, owing to a similar
82 scenario, the probability of having a good permeability in the reservoir section above the water-oil
83 contact can be probably underestimated. Calculated permeability is affected by its estimation accuracy
84 (Wu, Keliu and Li, X, 2013). The calculated permeability care can be subdued to some uncertainties
85 regarding its estimation exactitude. This kind of statement might be proofed by water-wet rocks and
86 high salinity formations (Elraies, Khaled Abdalla and Yunan, Mat Hussin, 2007).

87 The general complexity for the reservoir characterization related to permeability prediction especially
88 in the non-cored borehole section, is conducted towards a variety of methods, which can be executed.
89 Investigating on permeability and porosity characteristics, with regards to geological properties of the
90 rocks, might carry considerable reserves. Texture and structure factors with mineral composition and
91 their distribution (arrangement, packing, sorting distribution), remain an essential impact regarding
92 uncertainties on rock typing and degree of heterogeneities statements (Benzagouta, Mohammed, 2015).
93 Conversely, making use of parameters recorded from the formation evaluation, ambiguity concerns
94 might be improved for sustaining the decrease in rock typing uncertainties (Mohammad Emami Niri and
95 David Lumley, 2014, Pirrone, M. et al., 2014).

96 Similar statement is well known in the Lower Shaly – Triassic Sandstone Formation (TAG-I Formation,
97 Algeria), where, the main characteristics controlling rock typing uncertainties, can be owed to rock
98 solids textural and fractional compositional. In addition, contribution is expected from fluid flow filling
99 pores and its properties.

100 For similar purposes and to clear out various doubts for the case study investigation, conducted tasks
101 can be set as follow:

- 102 • Rock typing identification based on integrating, analyzing and synthesizing data from well logs
103 and core analysis.
- 104 • Rock typing identification related to the volume of shale estimated from gamma-ray (GR),
105 hydraulic units, capillary pressure profile, and saturation height function.
- 106 • Finding out relation between completed classification process using FZI method
107 and permeability models specified for each rock type.
- 108 • Anticipating the determination of FZI from well logs application using the empirical model and
109 non-linear regression approaches.
- 110 • Final objective is to calculated permeability from FZI based on rock typing classification in
111 reservoir sections.

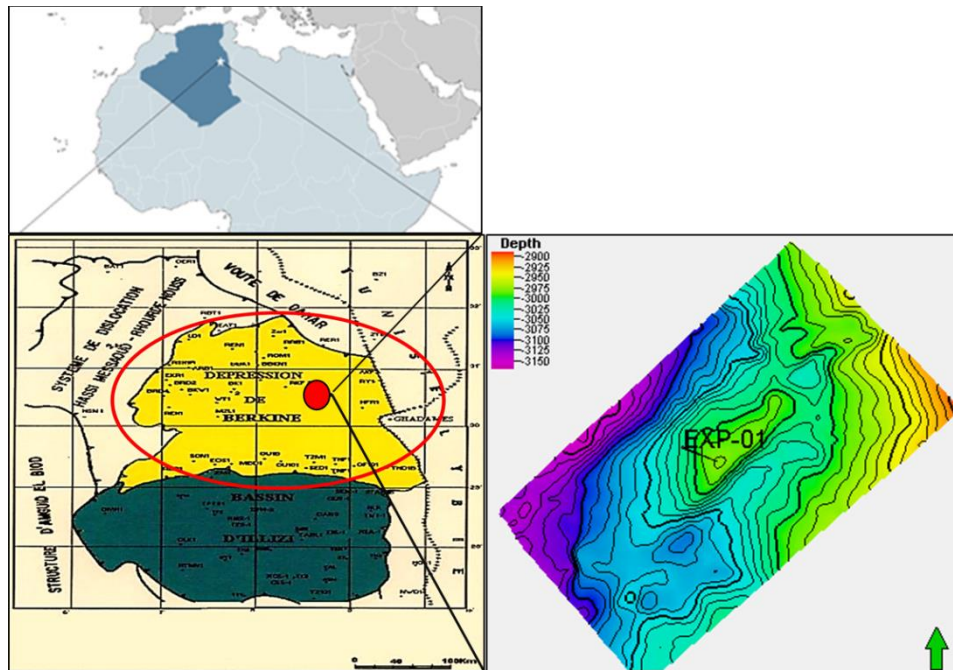
112 **2. Field description and Well presentation**

113 As part of the Saharan Platform, the Berkine Basin is located in South-Eastern Algeria, between latitude
114 29 degrees and 33 degrees North and longitude 5 degrees and 9 degrees East (Figure 1). It is limited to
115 the North by the southern border of the Dahar Mole, to the south by the Mole D'Ahara which separates
116 it from the Illizi basin, to the East by the Tunisian – Libyan borders and finally to the West by the
117 structural extension North of the Amguide – El Biode – Hassi Messaoud Mole. The Berkine basin is of
118 intracratonic type with a total area is 102,395 km² (Souadnia, S. and Mezghache, H., 2009).

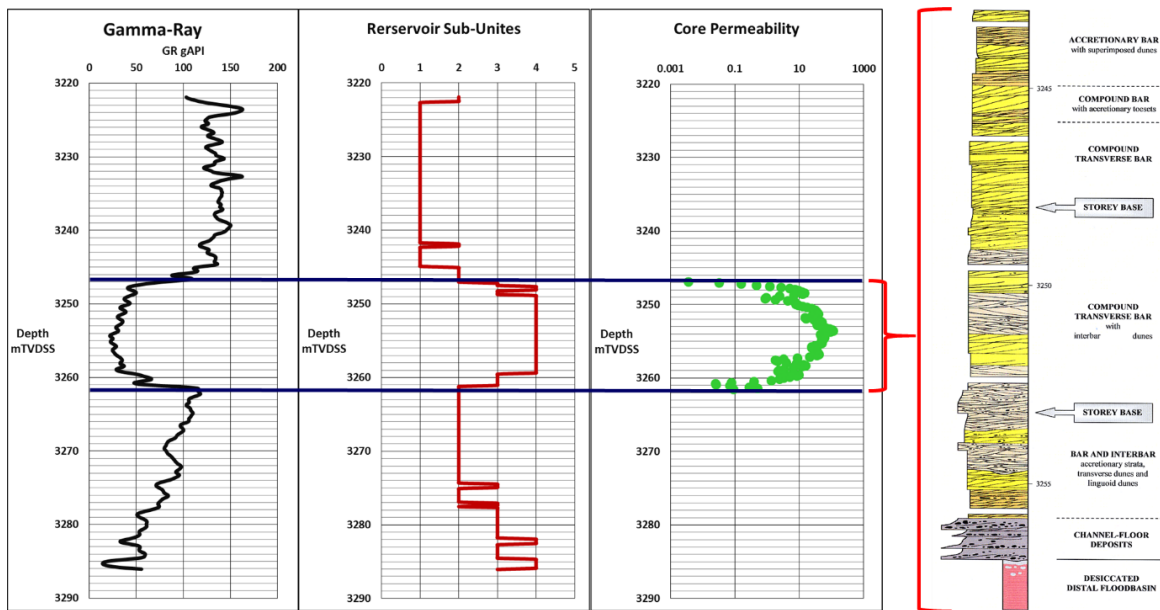
119 The EXP-01 exploration well has been drilled in the Berkine oil field Basin for assessing the H-C
120 potential of sandstone part within the Triassic Lower Sandstone Clay TAG-I stratigraphic column
121 (Figure 2) . A 15 m core thickness was picked up between 3247 m TVDSS (true vertical depth subsea)
122 and 3262 m TVDSS. A total Core recovery was achieved without any loss (100% recovery). The core
123 height has been found covering the entire reservoir targeted section. The core section has been described
124 from sedimentological and petrographical points (figure 2). Results, based on the stratigraphic log of
125 the core interval and the whole borehole section, indicate a detrital sandstone lithology dominance,
126 which may be split up into different facies deposits according to Turner, P. et al., 2001 (figure2). From
127 sedimentological point of view, the Berkine basin deposits have been found of braided to meandering
128 fluvial environmental deposits (Turner, P. et al., 2001).

129 Reservoir characteristics have also been found of relatively up to good with porosity varying from 7 to
130 20 % and the permeability from 1 millidarcies to 850 millidarcies (mD). The PVT (Pressure, Volume,

131 and Temperature) analysis has indicated light oil, with a gravity of 40.4 API (Souadnia, S. and
 132 Mezghache, H., 2009).



133
 134 Figure 1: The localization of the study area and Well position (Souadnia, S. and Mezghache, H., 2009)



135
 136 Figure 2: Stratigraphic column for reservoir coring section (Turner, P. et al., 2001).

137 **3. Core Samples porosity and permeability measurements**

138 42 conventional core measurements have been selected from the reservoir interval (essentially the Net
 139 pay sections) in the first exploration borehole. Porosity and the permeability are targeted in the
 140 assessment purpose. Six special core measurements with mercury intrusion-porosimetry have been
 141 selected to define capillary pressure (Pc). The experiments have been realized in the laboratory. Prior to
 142 petrophysical characteristics measurements, the core plugs underwent the following laboratory
 143 procedures, at ambient conditions.

- 144 - Cleaning procedure
- 145 - Helium derived porosity
- 146 - Klinkenberg corrected gas permeability

147 **3.1 Cleaning and drying**

148 The preferred Routine core analysis (RCA) method for cleaning of plugs has been the hot Soxhlet reflux
 149 cleaning with methanol and toluene as the most used cleaning liquids, followed by chloroform/methanol
 150 and finally methanol, Extended cleaning for 2-4 weeks are often necessary depending the core
 151 permeability. Drying is normally done at 105-110 °C to remove adsorbed humidity and obtain the most
 152 accurate porosity and grain density figures.

153 **3.2 Helium porosity determination**

154 Porosity was determined by helium injection using a Boyle's law porosimeter. The bulk volume was
 155 measured using the immersion in the Mercury technique. The method used for porosity calculation is
 156 based on consolidated rocks. The method was based on some cylindrical plugs allowing the volume
 157 calculation (bulk volume) (irregular shapes are not accurate): length and diameter have to be measured
 158 accurately.

159 We can determine the solid volume or the pore volume by saturation subsequent to air evacuation using
 160 a vacuum pump. Total Saturation of the sample is accomplished by a fluid of known density. The sample
 161 is weighted (Ww). Then Sample is dried (furnace). The difference in weight between saturated and dry
 162 samples can give us the pore volume according to fluid density (generally when it consists of water:
 163 water density = 1 g/cm³. The porosity is expressed as:

$$164 \text{ Porosity } (\phi) = \frac{\text{Volume of Pore } (V_p)}{\text{Total volume of rock } (V_b)} * 100 \quad (1)$$

164 **3.3 Klinkenberg corrected gas permeability**

165 The general measurement of permeability (K) is based on the type of fluid, its viscosity, pressure
 166 difference between the inlet and outlet, sample section and its length. The permeability measurement
 167 has been taken in the company laboratory. It has been measured by using core cylindrical samples
 168 according to the process: A fluid of known viscosity (μ) is pumped through a rock sample of known
 169 cross-sectional (A) area and length (L). The pressure drop across the sample is measured through
 170 pressure gauges ($\Delta p = P_{inlet} - P_{outlet}$).

171 The Darcy's Law as formulated by Muskat and Botset is as follows (MUSKAT, 1931):

$$172 \quad Q = \frac{k * (P_1 - P_2) * A}{\mu * L} \quad (2)$$

172 Where:

173 Q : Rate of flow (cm³/s)

174 k : Permeability (Darcy)

175 $(P_1 - P_2)$: Pressure drop across the sample (atmosphere)

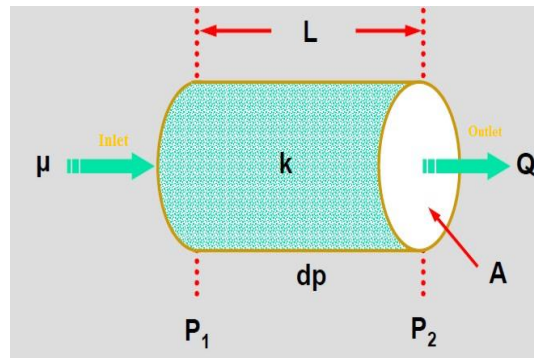
176 A : Cross-sectional area of the sample (cm²)

177 μ : Viscosity of fluid (cP)

178 L : Length of the sample (cm)

179 Nothing that, in the form shown above, we assume that the equation (2) is occurring without any
 180 chemical reaction between the fluid and the rock, with only one fluid phase (after cleaning procedure).

181 The permeability measurement procedure can be illustrated by the schematic diagram below (Figure 3):



182

183 Figure 3: General permeability measurement scheme According to Darcy Law (Zand, A. et al., 2007)

184 Detailed information on the purpose of these procedures of laboratory measurements and various steps,
 185 for the core use, were figured out from laboratory core analysis and guides (McPhee et al., 2015, William
 186 Lyons, et al., 2015).

187 **4. Rock Typing; Identification and assignment**

188 In reservoir engineering, rock classification can be made on the basis of hydraulic unit identification,
 189 planned for fluid circulation ability and determination (Attia, M. Attia and Shuaibu, Habibu , 2015).
 190 These hydraulic units (HU) are used for modeling parameters such as permeability (K) (Mahjour, S.K.
 191 et al., 2016) in order to optimize simulation time. Rock typing is determined on the basis of reservoir
 192 petrophysical properties, porosity – permeability cross plot, capillary pressure curves, in addition to
 193 water saturation height function profiles. Generally, the determination of these parameters will help to
 194 define different rock classes and their contribution potential towards predicted recovery. Conducting
 195 similar research consists on making use of data from different sources (well logs and core data) to
 196 support identification of the different rock types. As mentioned previously, the static behavior
 197 (Lithology, rock type and physical properties) can be gathered to dynamic behavior (petrophysical
 198 parameters relationship and capillary pressure effect). In that principle, defined rock types must be
 199 calibrate in terms of the following defined setting:

- 200 • Lithofacies: the same type of rock in terms of lithology.
- 201 • Petrofacies: the process is based on the classification of cores data into sets having the same
 202 hydraulic unit (FZI method), the same pore size and similar capillary pressure profile.

203 **5. Application for the case study: Results and Discussion**

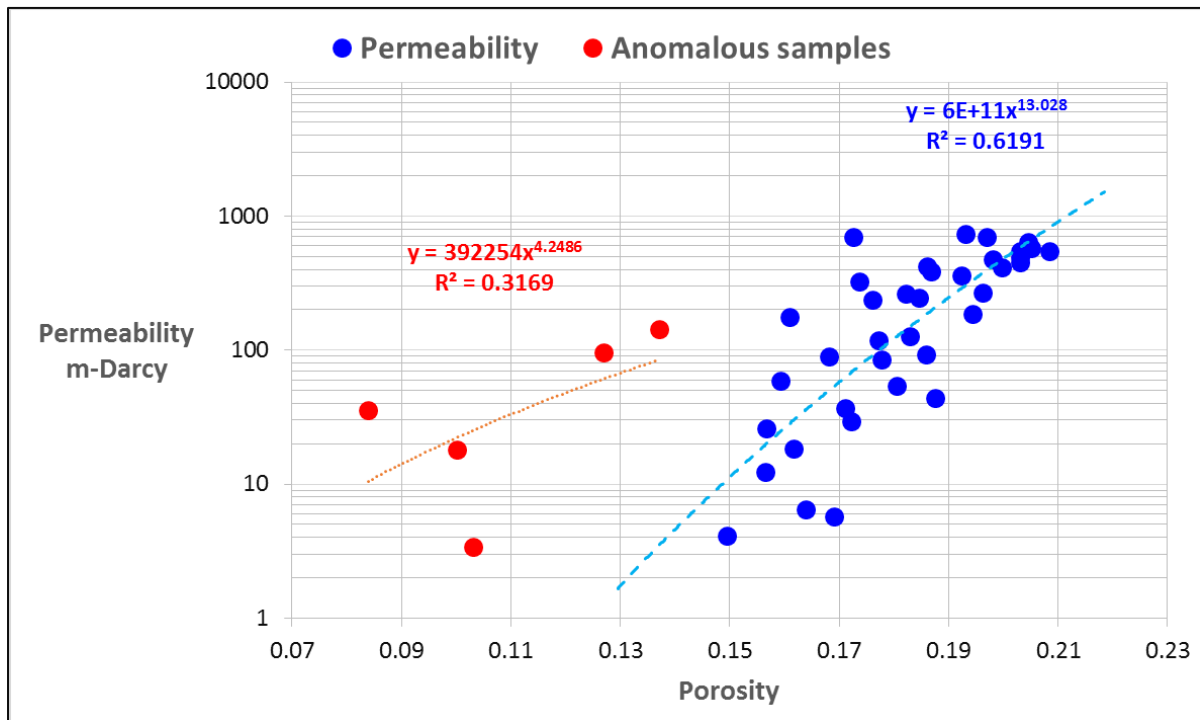
204 In the case study, exploitation of cores, coming from the first explored borehole in the Hassi - Berkine
 205 oil field (Algeria), has been used for rock typing identification. These cores have been characterized on
 206 the basis of porosity and permeability properties. These factors are considered as the main indicators for
 207 the reservoir classification process. Before going through this process, a plotting permeability versus
 208 porosity relation is required and becomes essential. According to permeability porosity distribution, and
 209 regarding the porosity evolution, two groups of samples distribution were set up main (normal) samples
 210 and anomalous samples. In addition, a relation between permeability and porosity was also established
 211 (Figure 4).

212 **5.1 Permeability Porosity relationship**

213 Permeability versus porosity relation, recorded from core analysis, presents a non – uniform cloud over
 214 which a representative mathematical model is privileged. This predicted model can be set on the basis
 215 of a best-provided correlation coefficient. Providentially, the rock type classification procedure begins

216 by removing core results located out of the main set of points. Permeability versus porosity recorded
 217 outcomes from core analysis indicates the best fit line, crossing a group with a correlation coefficient of
 218 0.62 (Figure 4). This low value of the correlation coefficient provides a considerable margin of error.
 219 All calculations, depending directly or indirectly on absolute permeability, will be overestimated.

220 Therefore the numerical simulation model does not represent the real field performance. In that purpose,
 221 the application of the HFU parameter becomes necessary to predict the various reservoir rock types
 222 (RRT) and the degree of reservoir heterogeneities. With reference to parameters control, this request
 223 will possibly improve the absolute permeability calculation and subsequently extended to the uncored
 224 sections, thus, this prediction will be used to decrease the uncertainties surrounding the uncored zones.



225
 226 Figure 4: A cross plot indicating permeability versus porosity where heterogeneity is illustrated
 227 through a predetermined interval of distribution

228 **5.2 Data availability and Quality Control (QC)**

229 To carry out a complete study on reservoir rock types classification in the cored and uncured wells, a
 230 data preparation must be carried out, and presented as follows;

- 231 • Core data in cored wells, and well logs data in all wells should be prepared and quality
 232 controlled.
- 233 • Quality insurance of core data should be necessary; all cores destroyed during the sampling
 234 should be removed.
- 235 • Porosity estimation from well logs should be calibrated to that calculated from cores with
 236 consideration of the overburden phenomenon.
- 237 • Core data depth correction must be adjusted.

238 **5.3 Rock Typing**

239 According to Chehrazi, A. et al., (2011), reservoir rock typing is a process of classifying reservoir rocks
 240 into distinct units. From a geological point of view, it is characterized by similar geological conditions
 241 deposited in the same sedimentary environment and undergone through similar diagenetic alterations.

242 From the reservoir engineering point of view, it is characterized by identical fluid flow properties. Based
 243 on these definitions, given rock type can be imprinted by a unique permeability - porosity relationship,
 244 capillary pressure profile and saturation height functions above free water level (HFWL).

245 In the case study, reservoir rock types identification is the process by which rocks are regrouped in
 246 specific sets and are calibrated in terms of lithofacies and petrofacies. In the case study, two principal
 247 steps have been considered to define reservoir rock types:

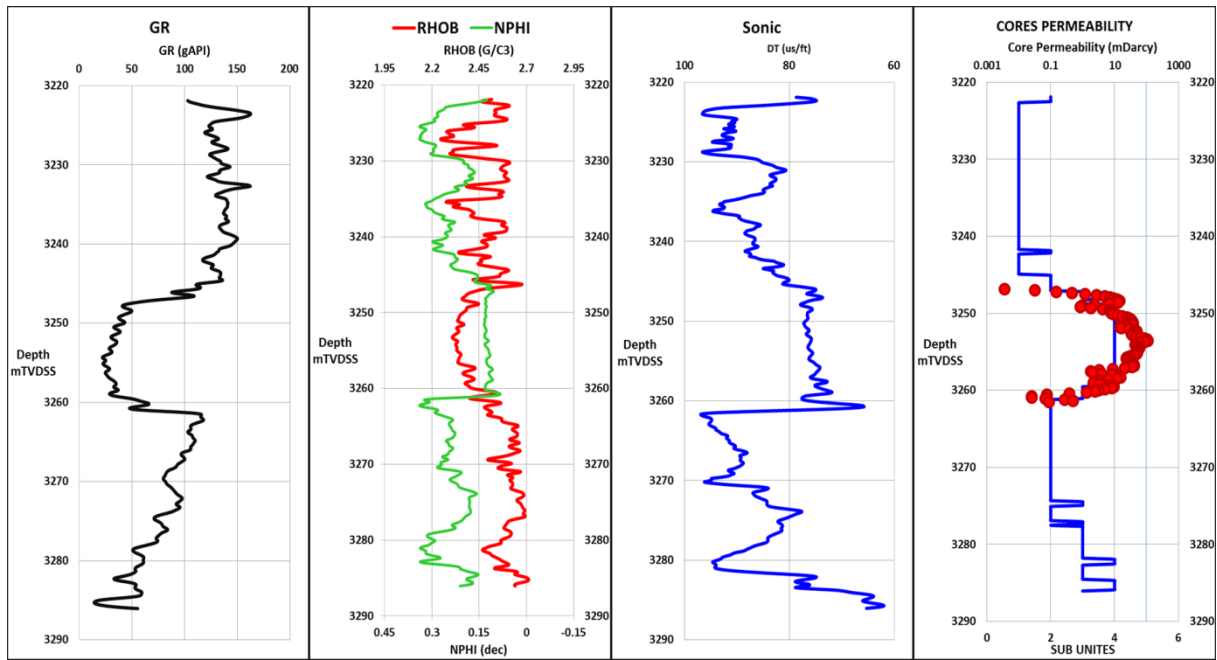
248 **5.3.1 Lithofacies identification**

249 Lithofacies determination is derived from the description of core and cuttings obtained during the
 250 drilling phase. The different lithological units are grouped, as mentioned previously, to similarities in
 251 rock composition, texture, and sedimentary structures. Therefore, each lithofacies should be associated
 252 with a specific Rock type.

253 According to the carried out description of the cores and the cutting, the whole material consists on
 254 detrital deposits. Therefore, shaliness or clay content parameter constitutes a basic parameter to be used
 255 for splitting up between the different facies. The availability of Gamma ray records is a valid tool for
 256 this function (Turner, P. et al., 2001, Benzagouta, M.S. et al., 2001). For that purpose, the gamma-ray
 257 log has been used, as the main source for lithofacies identification and classification, matching the
 258 defined lithofacies from core description and cutting (Table 1). Based on this perceptive concept, five
 259 lithofacies were defined in Hassi Berkine Oil Field. Two defined types of lithofacies: organic-rich shale
 260 and shales are considered as non-reservoir with regards to the others. Plotting core permeability versus
 261 porosity for defined reservoir subunits shows that three lithofacies could be considered as probable
 262 reservoir efficient facies; Shaly sandstone, sandstone and clean sandstone (Figure 5).

Commun lithological description		Lithofacies	Codes
Non Reservoir	Dark clay rich in organic matter content	Organic-rich Shales	1
	Greenish clay deposits	Shales	
Reservoir (net pay)	Heterogeneous lithic facies alternating with fine to very fine sand and clay with some pebbles including coal fragments and some mud-clasts.	Shaly Sandstone	2
	fine to medium sandstone	Sandstone	3
	Medium to coarse clean sandstone	Clean Sandstone	4

263 Table 1: Table showing the main lithofacies characteristics in the considered reservoir according to
 264 Asquith, G. with Gibson C., 1983, Turner, P. et al., 2001 and Benzagouta, M.S. et al., 2001



265

266 Figure 5: Well log interpretation based on GR classification indicating the location of core data in
 267 reservoir zones

268 **5.3.2 Petrofacies determination**

269 In this case study, Amaefule, J. O. et al., (1993) method was applied to identify hydraulic units. This
 270 latter parameter could be presented by a unique permeability – porosity relationship. Results are
 271 indicated in Figure 6. This method deals with the rock quality index (RQI) versus normal porosity (ϕ_z).
 272 The calculation of these parameters has been achieved graphically based on the unit slope. As a result,
 273 six hydraulic units revealing six dynamic curve behaviors were obtained (Figure 6a).

274 For each hydraulic unit, permeability factor was obtained from FZI_{mean} and effective porosity using
 275 the equation below (equation 3) (Enaworu, E. et al., 2016). Consequently, various rock types are laid
 276 down (Figure 6b).

$$k = 1014 * FZI_{mean}^2 \left[\frac{\phi_e^3}{(1 - \phi_e)^2} \right] \quad (3)$$

277 Then, the units were modeled by a linear, logarithmic, exponential and power-law in order to determine
 278 the best representative equation corresponding to each hydraulic unit (Table 2, Figure 6c). The choice
 279 of a mathematical model, representing the same set of points, is coupled to the correlation coefficient.
 280 This correlative coefficient is used to measure the strength of the relationship between the two essential
 281 petrophysical parameters: porosity and permeability. Figure 6d indicates, that the best correlation
 282 between the cited type of modeled and actual cores measurements permeability, with a high degree of
 283 accuracy, is set through the correlation coefficient value of 0.97.

284 In addition to the identification of the hydraulic units, six collected samples, from the reservoir area (net
 285 pay section or probable efficient section), were used to calculate the capillary pressure (P_c) by the
 286 Mercury Injection Capillary Pressure experiment (MICP). The principle is to evaluate the capillary
 287 behavior of these samples as a function of defined hydraulic units. Figure 7a is a graphical analysis of
 288 capillary pressure versus saturation: each capillary pressure value corresponds to a respective hydraulic
 289 unit. It is found that rock types RT-5 and RT-6 have the same initial water saturation (Figure 7b). This

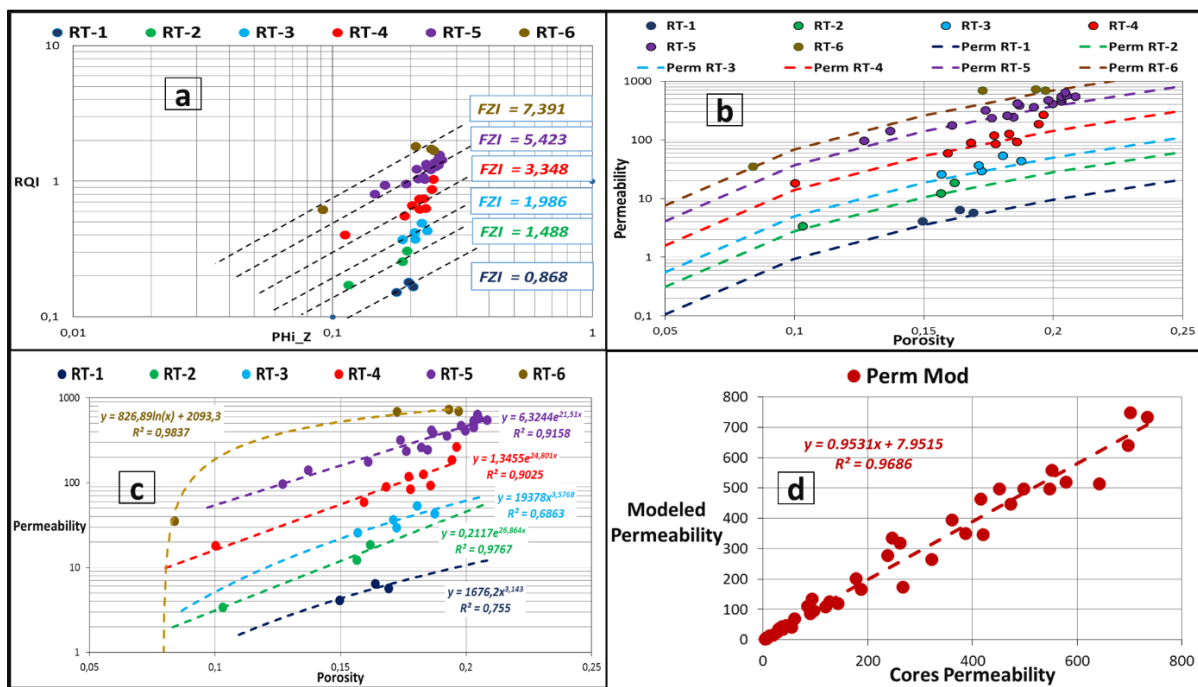
290 can be a support to set together rock types RT-5 and RT-6 in the same rock type, sustaining a consistent
 291 classification, in terms of hydraulic units and capillary pressure profiles. Consequently, the
 292 petrophysical rock types will be summarized in five rock types RT-1, RT-2, RT-3, RT-4 and RT-5bis
 293 (RT-5 and RT-6).

294 According to the outcomes, from the figures 6a and 6b, the presence of more than one hydraulic unit
 295 and dissimilarities in the capillary pressure profiles can be ascribed to the heterogeneity of depositional
 296 environment change or lithological distribution variation. For supporting this hypothesis, pore size
 297 distribution has been calculated from capillary pressure and presented in figure 8.

298 Graphical analysis shows that pore throat is of mostly macroporous type, with a pore throat radius
 299 fluctuating between 2.5 and 10 microns meter, with minor variations of mesoporous (0.5 - 2.5 microns
 300 meter) and microporous category (0.2 - 0.5 microns meter).

301 Accordingly, the reservoir rock quality type can be determined according to factors such as porosity,
 302 permeability, hydraulic unites, capillary pressure and pore throat radius. The determination of the values
 303 of this last parameter can be an effective device to assess the heterogeneity degree. Based on pore size
 304 distribution profiles, reservoir facies could be considered as relatively homogenous along the field
 305 sections. The presence of more than one hydraulic unit can be related to variation in lithological facies
 306 distribution.

307 In the case study and as results, Hassi Berkine oil field reservoir rock types (RRT) have been classified
 308 into five lithofacies and six petrofacies, the results are shown in Table 3.



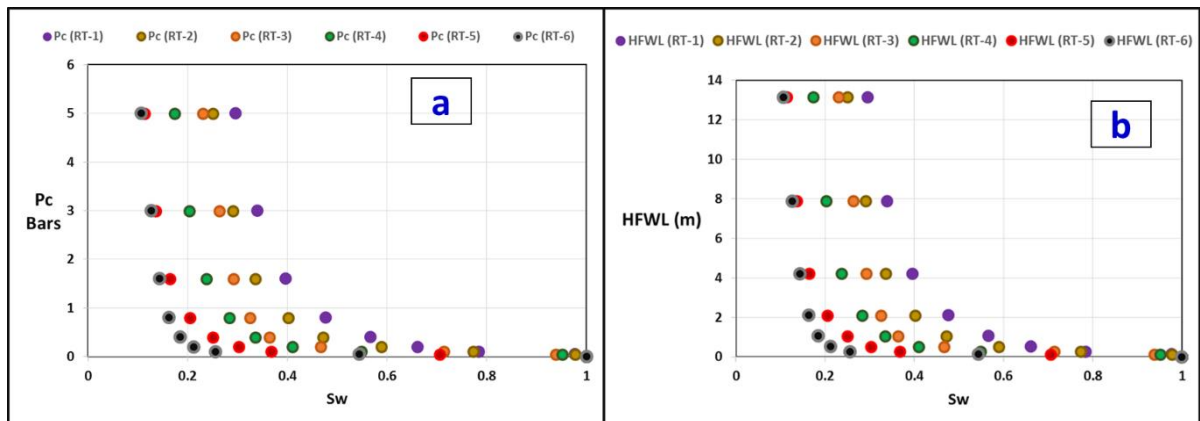
309
 310 Figure 6: Permeability vs. porosity with the obtained different curves and correlation coefficient:
 311 Different clusters have come out with various hydraulic units leading to different rock typing
 312 (Amaefule, J. O. et al., 1993)

313
 314
 315

Rock Types	FZI Intervals	Function	Modelled Permeability	Correlation Coefficient
RT-1	FZI < 0.9205	Exponential	$0.2258 * \exp^{19.677 * \emptyset}$	0.7439
		Linear	$98.195 * \emptyset - 10.353$	0.6992
		Logarithmic	$15.698 \ln(\emptyset) + 34.147$	0.7109
		Power	$1676.2 * \emptyset^{3.143}$	0.755
RT-2	0.9205 < FZI < 1.8033	Exponential	$0.2117 * \exp^{26.864 * \emptyset}$	0.9767
		Linear	$220.67 * \emptyset - 19.566$	0.8882
		Logarithmic	$28.369 * \ln(\emptyset) + 67.677$	0.8785
		Power	$8856.8 * \emptyset^{3.464}$	0.9719
RT-3	1.8033 < FZI < 2.7785	Exponential	$0.9859 * \exp^{20.833 * \emptyset}$	0.684
		Linear	$755.16 * \emptyset - 93.136$	0.6166
		Logarithmic	$129.53 * \ln \emptyset + 256.01$	0.6175
		Power	$19378 * \emptyset^{3.5768}$	0.6863
RT-4	2.7785 < FZI < 4.5697	Exponential	$1.3455 * \exp^{24.801 * \emptyset}$	0.9025
		Linear	$1876.7 * \emptyset - 205.29$	0.5569
		Logarithmic	$249.19 * \ln(\emptyset) + 559.96$	0.4901
		Power	$43352 * \emptyset^{3.4433}$	0.8683
RT-5	4.5697 < FZI < 6.7378	Exponential	$6.3244 * \exp^{21.51 * \emptyset}$	0.9158
		Linear	$6095.8 * \emptyset - 750.12$	0.7979
		Logarithmic	$992.79 * \ln(\emptyset) + 2061.4$	0.7575
		Power	$143020 * \emptyset^{3.5654}$	0.9007
RT-6	FZI > 6.7378	Exponential	$3.7498 * \exp^{27.811 * \emptyset}$	0.9616
		Linear	$6280.3 * \emptyset - 473.06$	0.9658
		Logarithmic	$826.89 * \ln(\emptyset) + 2093.3$	0.9837
		Power	$325345 * \emptyset^{3.6651}$	0.9812

316

Table 2: Table summarizing the classification of rocks based on FZI method

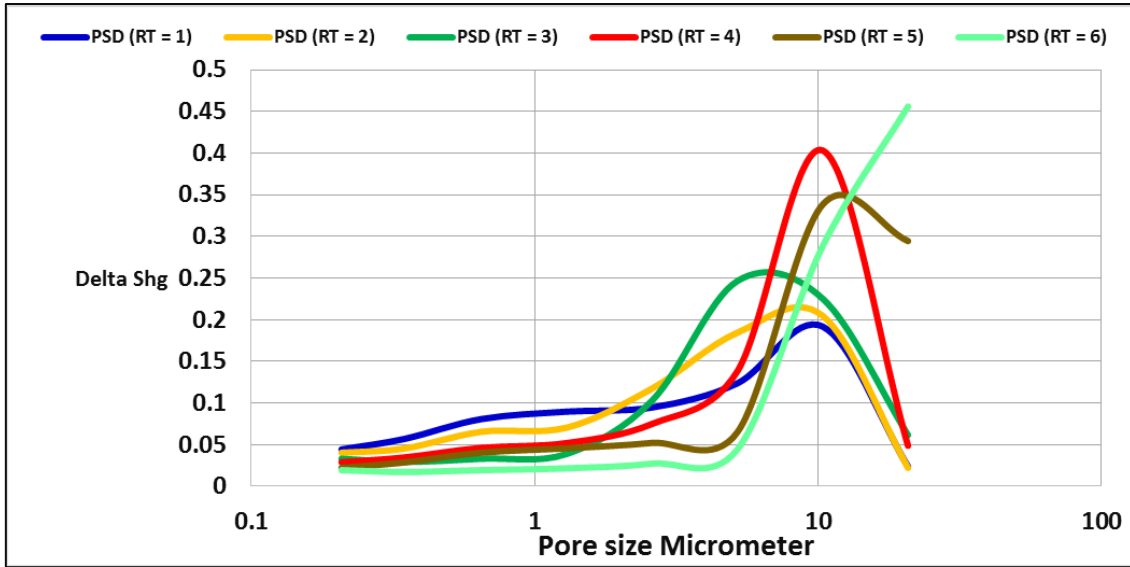


317

318

319

Figure 7: Capillary pressure (Pc) and Saturation height function (HFWL) profiles for each reservoir rock type (RRT)



320

321

Figure 8: Pore size distribution deduced from capillary pressure (MICP method)

Reservoir/Non Reservoir	Lithofacies	Petrofacies	
		RT0	Non Reservoir
Reservoir	Organic rich shales	RT0	Non Reservoir
	Shales		
	Shaly-Sandstone	RT-1	FZI < 0.9205
		RT-2	0.9205 < FZI < 1.8033
	Sandstone	RT-3	1.8033 < FZI < 2.7785
RT-4		2.7785 < FZI < 4.5697	
Clean Sandstone	RT-5bis	FZI > 4.5697	

322

Table 3: Reservoir rock types (RRT) Classification

323 5.4 Permeability Estimation for Non-Cored Section

324 According to the flow zone indicator method applying for rock typing identification, the permeability
 325 models for each rock type has been established and defined in the cored section (Enaworu, E. et al.,
 326 2016). In order to calculate the permeability for the non-cored section, the determination of FZI should
 327 be necessary. For that reason, nonlinear regression methods have been carried out to calculate FZI in
 328 the non-cored section.

329 For accomplishing the precedent purpose, well logs data should be used for analysis and interpretation.
 330 It will provide an approach allowing non-cored section classification into reservoir rock types. Thus, for
 331 such setting FZI and Permeability models could be applied.

332 In the case study, the volume of shale (V_{sh}) determination has subdivided the reservoir zone into four
 333 sub-zones. The sub-zones have been defined as Sand, Shaly-Sand, Sandy-Shale, and Shale (Table 4).
 334 Cores are located in the sandstone (unite 4) and shaly-sand (unite 3) zones (Figure 5, Table 4).

335 According to Tanmay Chandra (2008), FZI can be calculated from the combined use of well log data
 336 such as Gamma-ray (GR), NPHI, RHOB, and Sonic (DT) (Equation 4):

$$FZI = f(GR, NPHI, RHOB, DT) \quad (4)$$

337

GR Max	162.7971	GR readings	Reservoir Subunits	
GR Min	14.0944	GR < 1/2 GR Mid	Sandstone & Clean Sandstone	4
GR Mid	88.44575	1/2 GR Mid < GR < GR Mid	Shaly Sandstone	3
1/2 GR Mid	44.222875	GR Mid < GR < 3/2 GR Mid	Shale	2
3/2 GR Mid	132.668625	GR > 3/2 GR Mid	Organic Rich Shale	1

338 Table 4: Clay evolution (V_{sh}) in the reservoir based on GR readings

339 In this study, our approach is focusing on the determination of the normalized FZI from combined use
340 of well log data such as Gamma-ray (GR), NPHI, RHOB, and Sonic (DT). Based on this understanding,
341 empirical modeling (EM) was applied to create models based on the experimental data to predict the
342 normalized FZI model calculated from well logs and accordingly used in permeability calculation
343 through the application of the reservoir rock typing process. In order to achieve this objective, several
344 models were produced on the basis of the combination of mathematical functions such as; linear,
345 exponential, logarithmic, power and rational functions using conventional well logs such as; Gamma-
346 ray, NPHI, RHOB, and DT. The best mathematical model must be related to the optimal subject function
347 and characterized by its specific logs. The objective function or the optimized goal of the proposed
348 model consists essentially to minimize the quadratic error. This later will be between the calculated and
349 the observed normalized FZI as mentioned in the equation 5:

$$Obj_{func} = minimize \left(\sum_{i=1}^n (FZI_{obs}^* - FZI_{calc}^*)^2 \right) \quad (5)$$

350 Where:

351 Obj_{func} : The objective function

352 FZI_{obs}^* : Observed normalized FZI factor

353 FZI_{calc}^* : Calculated normalized FZI factor

354 n : The number of cores presented in this study ($n = 42$)

355 and normalized observed FZI (FZI_{obs}^*) has been calculated by applying Shier, D.E., (2004) formula as:

$$FZI_{obs}^* = \frac{FZI - FZI_{min}}{FZI_{max} - FZI_{min}} \quad (6)$$

356 Where FZI , FZI_{min} and FZI_{max} are considered from core data.

357 We note that FZI^* is constrained by the rock lithofacies (Shaly-Sandstone and Sandstone & clean
358 Sandstone subzones), this means that each lithofacies has a specific mathematical model.

359 In this investigation, in order to solve the nonlinear optimization problem and compute the optimum
360 model parameters according to the chosen subject function, the Generalized Reduced Gradient (GRG)
361 method was performed (Maia A. et al., 2017). The mathematical models of normalized FZI (FZI_{calc}^*)
362 for shaly-sandstone and sandstone & clean sandstone subzones were developed. They were performed
363 on the basis of several scenarios carried out on the observed normalized FZI coming from cores and
364 normalized FZI estimated from normalized well logs, RHOB* and DT*. NPHI* has been used as a
365 parameter, but it has not led to good results. Thus, the mathematical models deduced for the two
366 subzones are correspondingly:

367 - Shaly-Sandstone;

$$FZI_{calc}^* = 0.312739 * \ln(RHOB^* + 1.163084) + 1.105386 * \ln(DT^* + 0.789186) \quad (7)$$

368 - Sandstone & clean Sandstone;

$$FZI_{calc}^* = \frac{1.342524}{-1.00692 + 1.408993 * e^{4.16757 * RHOB^*}} \quad (8)$$

369 Where $RHOB^*$ and DT^* are normalized parameters and are calculated by Shier, D.E., (2004):

$$Normalized_{log} = \frac{Reading\ Value - Min\ Value}{Max\ value - Min\ Value} \quad (9)$$

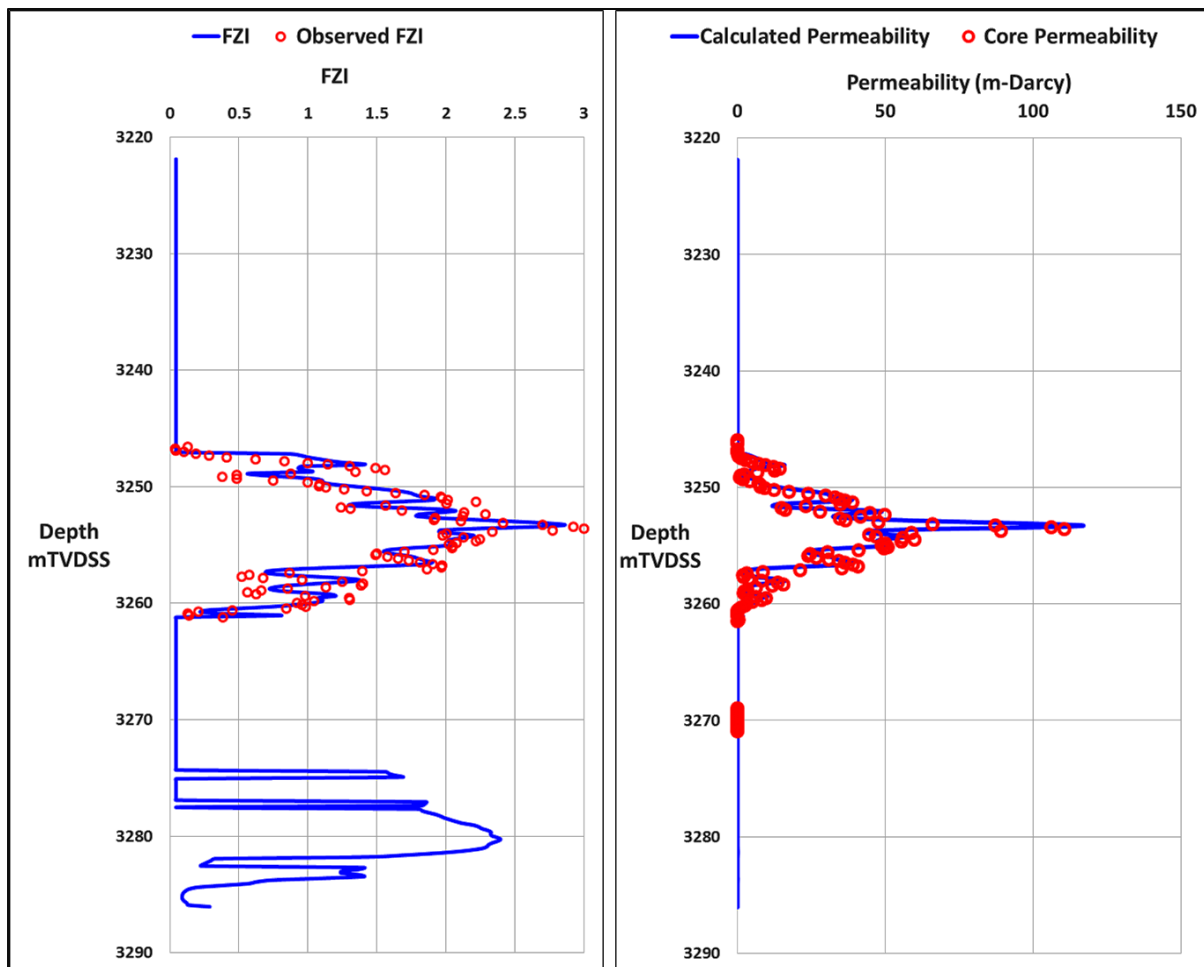
370 Based on the equation 6, the FZI log is calculated from the normalized FZI and stated as follows:

$$FZI_{log} = FZI_{calc}^* * (FZI_{max} - FZI_{min}) + FZI_{min} \quad (10)$$

371 For the permeability calculation, reservoir rock types were classified on the basis of the FZI values, in
 372 which a permeability model was defined for each rock type (Table 5). The results presented in figure 9
 373 indicate a relative fine correlation between calculated and observed parameters (FZI and Permeability),
 374 and therefore, these inferred models can be used to calculate the permeability in the non-cored wells.

Rock Types	FZI Intervals	Function	Modelled Permeability	Correlation Coefficient
RT-1	$FZI < 0.9205$	Power	$1676.2 * \emptyset^{3.143}$	0.755
RT-2	$0.9205 < FZI < 1.8033$	Exponential	$0.2117 * exp^{26.864 * \emptyset}$	0.9767
RT-3	$1.8033 < FZI < 2.7785$	Power	$19378 * \emptyset^{3.5768}$	0.6863
RT-4	$2.7785 < FZI < 4.5697$	Exponential	$1.3455 * exp^{24.801 * \emptyset}$	0.9025
RT-5bis	$4.5697 < FZI < 6.7378$	Exponential	$6.3244 * exp^{21.51 * \emptyset}$	0.9158
	$FZI > 6.7378$	Logarithmic	$826.89 * \ln(\emptyset) + 2093.3$	0.9837

375 Table 5: Table summarizing the permeability models for each rock type



376

377

Figure 9: FZI and Permeability profiles calculated from well logs data

378

6. Conclusion

379

- Rock typing can be defined as integration and analysis of data from boreholes and core analysis.
- Rock typing determination can be due to various factors leading to various modifications.
- Lithofacies process is a helpful tool that can be used to link core data to Well log column data.
- Identification of hydraulic unit parameters such as HFU and FZI can be a vital compilation between the real cores and petrophysical characteristics.
- Capillary pressure and saturation height function are influencing factors regarding reservoir rock typing classification.
- Pore size distribution (PSD) could be introduced to identify the reservoir degree of homogeneity or heterogeneity.
- Uncertainties on data analysis with various obtained mathematical curves can be involved and useful to find out and support the correlation between hydraulic units issued from core data and well logs.
- The use of the classification process can be main concern for the permeability determination and its anticipation for each rock type.
- Similar investigation on reservoir characterization steps can be applied for other non-cored wells especially for boreholes set in the same structure and having broad-spectrum characteristics.

395

7. Conflict of interests

396

We attest and witness that there is no conflict of interest concerning the manuscript.

397 8. References

- 398 Al-Hajeri, M. et al. (2009). Basin and Petroleum System Modeling. *Oilfield Review Summer 2009: 21,*
399 *no. 2., 16.*
- 400 Amaefule, J. O. et al. (1993). Enhanced Reservoir Description: Using Core and Log Data to Identify
401 Hydraulic (Flow) Units and Predict Permeability in Uncored Intervals/Wells. *Society of*
402 *Petroleum Engineers. doi:10.2118/26436-MS, 205-220.*
- 403 Asquith, G. with Gibson C. (1983). *Basic Well Logging Analysis for Geologists, AAPG Methods in*
404 *Exploration Series number 3, Page 120.* Tulsa, Oklahoma USA: "The American Association of
405 Petroleum Geologists AAPG". 1982, Library of Congress. Schlumberger, Log Interpretation
406 Principles/Applications, Schlumberger, Wireline & Testing, Houston Texas.
- 407 Attia, M. Attia and Shuaibu, Habibu . (2015). Identification of Barriers and Productive Zones Using
408 Reservoir Characterization. *International Advanced Research Journal in Science, Engineering*
409 *and Technology, IARJSET. 2. 8-23. 10.17148/IARJSET.2015.21202, 16.*
- 410 Benzagouta, M.S. et al. (2001). Reservoir Heterogeneities, in Fractured Fluvial Reservoirs of the
411 Buchan Oilfield (Central North Sea). *Oil & Gas Science and Technology – Rev. IFP, Vol. 56*
412 *(2001), No. 4, 327 - 338.*
- 413 Benzagouta, Mohammed. (2015). Reservoir characterization: Evaluation for the channel deposits
414 sequence – Upper part using scanning electron microscope (SEM) and mercury injection
415 (MICP): Case of tight reservoirs (North Sea). *Journal of King Saud University - Engineering*
416 *Sciences, Volume 27, Issue 1, 57 - 62.*
- 417 Chehrazi, A. et al. (2011). Pore-facies as a tool for incorporation of small-scale dynamic information in
418 integrated reservoir studies. *Journal of Geophysics and Engineering, Volume 8, Issue 2, June*
419 *2011, Pages 202–224, 23.*
- 420 Elraies, Khaled Abdalla and Yunan, Mat Hussin. (2007). INVESTIGATION OF WATER BREAKTHROUGH
421 TIME IN NON-COMMUNICATING LAYERED RESERVOIR. *Journal of Chemical and Natural*
422 *Resources Engineering, 3 . pp. 12-18. ISSN 1823-5255, 7.*
- 423 Enaworu, E. et al. (2016). PERMEABILITY PREDICTION IN WELLS USING FLOW ZONE INDICATOR (FZI).
424 *Petroleum and Coal, 58 (6). pp. 640-645. ISSN 1337-7027, 6.*
- 425 Galard, Jean-Hector et Al. (2005). A case study on Redevelopment of a Giant highly fractured
426 Carbonate Reservoir in Iran based on integrated reservoir characterization and 3D modeling
427 studies. *SPE Middle East Oil and Gas Show and Conference, MEOS, Proceedings.*
428 *10.2118/93760-MS, 14.*
- 429 Holtz, M. H. (2002). Residual Gas Saturation to Aquifer Influx: A Calculation Method for 3-D
430 Computer Reservoir Model Construction. *SPE Proceedings - Gas Technology Symposium.*
431 *10.2118/75502-MS, 10.*
- 432 Mahjour, S.K. et al. (2016). Identification of Flow-units using Methods of Testerman Statistical
433 Zonation, Flow Zone Index, and Cluster Analysis in Tabnaak Gas Field. *Journal of Petroleum*
434 *Exploration and Production Technology volume 6, 577–592.*

435 Maia A. et al. (2017). Numerical optimization strategies for springback compensation in sheet metal
436 forming. *Computational Methods and Production Engineering, Research and Development,*
437 *Woodhead Publishing Reviews: Mechanical Engineering Series*, 51-82.

438 McPhee et al. (2015). *Core analysis : a best practice guide, Volume 64, 1st Edition, eBook, Chapter 5,*
439 *pp 181 - 266.* Radarweg 29, PO Box 211, 1000 AE Amsterdam, Netherlands: Elsevier.

440 Mohammad Emami Niri and David Lumley. (2014). Probabilistic Reservoir-Property Modeling Jointly
441 Constrained by 3D-Seismic Data and Hydraulic-Unit Analysis. *SPE Asia Pacific Oil and Gas*
442 *Conference and Exhibition, APOGCE 2014 - Changing the Game: Opportunities, Challenges*
443 *and Solutions (Vol. 1, pp. 368-382).* Australia: Society of Petroleum Engineers., 15.

444 MUSKAT, M. A. (1931). FLOW OF GAS THROUGH POROUS MATERIALS. *Journal of Applied Physics, vol.*
445 *1, no 1, 27 - 47.*

446 Pirrone, M. et al. (2014). Lithofacies Classification of Thin Layered Reservoirs Through the Integration
447 of Core Data and Dielectric Dispersion Log Measurements. *Society of Petroleum Engineers.*
448 *Society of Petroleum Engineers. doi:10.2118/170748-MS, 21.*

449 Richard C. Selley and Stephen A. Sonnenberg. (2015). *Elements of petroleum geology, Third Edition.*
450 525 B Street, Suite 1800, San Diego, CA 92101-4495, USA: Elsevier, page 488.

451 Shenawi, S. H. et al. (2009). Development of Generalized Porosity-Permeability Transforms by
452 Hydraulic Units for Carbonate Oil Reservoirs in Saudi Arabia. *SPE/EAGE Reservoir*
453 *Characterization and Simulation Conference, 19-21 October, Abu Dhabi, UAE, 16.*

454 Shier, D.E. (2004). Well log normalization: Methods and guidelines. *Society of Petrophysicists and*
455 *Well-Log Analysts, Petrophysics, Volume 45, Issue 03, 13.*

456 Souadnia, S. and Mezghache, H. (2009). *Caractérisation géologique et simulation du réservoir*
457 *d'hydrocarbure TAGI – HBNS, gisement Hassi Berkine Sud - à l'aide de méthodes*
458 *géostatistiques.* Annaba, Algeria: Université Badji Mokhtar.

459 Tanmay Chandra. (2008). Permeability estimation using flow zone indicator from Well log data. *7th*
460 *International Conference & Exposition on Petroleum Geophysics, 7.*

461 Turner, P. et al. (2001). Sequence stratigraphy and sedimentology of the late Triassic TAG-I (Blocks
462 401/402, Berkine Basin, Algeria). *Marine and Petroleum Geology, Volume 18, Issue 9, Pages*
463 *959-981.*

464 William Lyons, et al. (2015). *Standard Handbook of Petroleum and Natural Gas Engineering, Third*
465 *Edition, pp 957-961, eBook ISBN: 9780123838476,1822.* Gulf Professional Publishing.

466 Wu, Keliu and Li, X. (2013). A New Method to Predict Water Breakthrough Time in an Edge Water
467 Condensate Gas Reservoir Considering Retrograde Condensation. *Petroleum Science and*
468 *Technology. 31. 10.1080/10916466.2011.594830, 7.*

469 Zand, A. et al. (2007). A Simple Laboratory Experiment for the Measurement of Single Phase. *Journal*
470 *of Physical and Natural Sciences, Volume 1, Issue 2, 10.*

471